Articles in PresS. Am J Physiol Cell Physiol (August 15, 2012). doi:10.1152/ajpcell.00338.2011

VIP17/MAL Expression Modulates Epithelial Cyst Formation and Ciliogenesis

Vinita Takiar[1*], Kavita Mistry[1*], Monica Carmosino[1], Nicole Schaeren-Wiemers[2], Michael J. Caplan[1]

[1]Department of Cellular and Molecular Physiology, PO Box 208026, Yale School of Medicine, 333 Cedar Street, New Haven, CT 06520-8026 USA
[2]Department of Biomedicine, University Hospital Basel, 4031 Basel, Switzerland

* These authors contributed equally to this work

Running Title: VIP17/MAL Modulates Cyst and Cilium Formation

Corresponding Author: Michael J. Caplan, MD, PhD
Chair, Department of Cellular & Molecular Physiology
PO Box 208026
333 Cedar Street
New Haven, CT 06520-8026

Tel: (203) 785-7316
Fax: (203) 785-4951
Michael.Caplan@yale.edu

ABSTRACT:

The polarized organization of epithelial cells is required for vectorial solute transport and may be altered in renal cystic diseases. Vesicle integral protein of 17 kD (VIP17/MAL) is involved in apical vesicle transport. VIP17/MAL overexpression *in vivo* results in renal cystogenesis of unknown etiology. Renal cystogenesis can occur as a consequence of defects of the primary cilium. To explore the role of VIP17/MAL in renal cystogenesis and ciliogenesis, we examined the polarization and ciliary morphology of wild-type and VIP17/MAL-overexpressing MDCK renal epithelial cells grown in two-dimensional (2D) and three-dimensional (3D) cyst culture. VIP17/MAL is apically localized when expressed in cells maintained in 2D and 3D culture. VIP17/MAL-overexpressing cells produce more multi-lumen cysts compared to controls. While the distributions of basolateral markers are not affected, VIP17/MAL expression results in aberrant sorting of the apical marker gp135 to the primary cilium. VIP17/MAL overexpression is also associated with shortened or absent cilia. Immunofluorescence analysis performed on kidney sections from VIP17/MAL transgenic mice also demonstrates fewer and shortened cilia within dilated lumens ($p<0.01$). These studies demonstrate that VIP17/MAL overexpression results in abnormal cilium and cyst development, *in vitro* and *in vivo*, suggesting that VIP17/MAL overexpressing mice may develop cysts secondary to a ciliary defect.

KEY WORDS: cystogenesis, polycystic kidney disease, epithelial trafficking

61 **INTRODUCTION:**
62
63 Vesicular integral protein of 17 kD (VIP17/MAL), also known as myelin and
64 lymphocyte protein (MAL) and myelin vesicular protein of 17 kD (MVP), is a 17kD
65 proteolipid involved in the transport and delivery of carrier vesicles to the apical plasma
66 membrane domains of polarized epithelial cells.(9, 42, 61) Originally identified over 20
67 years ago through a search for genes that are differentially expressed during human T-cell
68 development, VIP17/MAL is also produced in oligodendrocytes and Schwann cells, and
69 in epithelial cells of the thyroid, kidney, stomach, and large intestine.(25, 32) In addition,
70 VIP17/MAL is expressed in cultured polarized epithelial cells, including the renal
71 MDCK cell line, a model system for studying epithelial polarity.(36, 61)
72 The VIP17/MAL gene encodes a non-glycosylated integral membrane protein
73 with four predicted transmembrane domains. In epithelial cells, VIP17/MAL is localized
74 predominantly at the apical plasma membrane.(19) VIP17/MAL contains multiple
75 hydrophobic segments and, in contrast to most other integral membrane proteins, is
76 highly soluble in organic solvents. This behavior accounts for the designation of
77 VIP17/MAL as a proteolipid. (1) Moreover, in all of the cell types in which it is
78 expressed, VIP17/MAL is present in glycolipid- and cholesterol-enriched membrane
79 (GEM) domains or "rafts".(25, 32, 35, 61) As incorporation into GEM domains at the
80 level of the TGN may be responsible for the apical sorting of a number of proteins, it is
81 possible that VIP17/MAL may facilitate the organization of apical cargo into
82 microdomains to facilitate their targeting and transport.(9, 42, 47, 61)
83 When VIP17/MAL levels are suppressed *in vitro* through treatment of cultured
84 epithelial cells with RNAi, the ordinarily apically-localized influenza hemagglutinin

85 protein accumulates in the Golgi complex with diminished apical expression and partial
86 missorting to the basolateral membrane.(9, 42, 61) In contrast, when VIP17/MAL is
87 overexpressed *in vitro*, net membrane delivery to the apical surface appears to be
88 enhanced, and as a consequence VIP17/MAL overexpressing MDCK cells have excess or
89 enlarged apical membranes.(9) When grown in three-dimensional culture, MDCK cells
90 in which VIP17/MAL expression has been decreased by RNAi manifest abnormal cyst
91 formation as well as atypical ciliogenesis.(53) These studies collectively suggest that
92 VIP17/MAL is involved in the accurate trafficking of a sub-group of proteins to the
93 apical surface in MDCK cells as well as in epithelial morphogenesis.

94 When VIP17/MAL is overexpressed under the control of its own promoter in
95 transgenic animals *in vivo*, the epithelial cells lining distal nephron segments in the
96 mouse kidney also appear to exhibit abnormal morphology. They manifest a
97 pseudostratified appearance with amplified apical membranes that balloon into the tubule
98 lumina. In addition, these animals develop renal cysts, although the histology of these
99 cysts differs from that characteristic of Autosomal Dominant Polycystic Kidney Disease
100 (ADPKD).(18) In these transgenic mice, renal expression of VIP17/MAL is greatest in
101 the collecting duct, although staining can also be detected in other tubule segments.(19,
102 23) The collecting duct also expresses aquaporin-2 (AQP2), the water channel that is
103 trafficked from an intracellular vesicular compartment to the apical plasma membrane in
104 response to the antidiuretic hormone, arginine vasopressin. VIP17/MAL co-localizes and
105 interacts with AQP-2 in the renal collecting duct.(23) In LLC-PK_1 cells, expression of
106 VIP17/MAL increases surface expression of AQP2 by decreasing the rate of the
107 channel's endocytic internalization.(23) Moreover, in cultured cells *in vitro*, vasopressin

108 induces the expression of VIP17/MAL, which may facilitate the apical trafficking or
109 retention of newly synthesized AQP2.(24) The VIP17/MAL-mediated increase in apical
110 AQP2 expression may be due to decreased endocytosis from the apical surface and/or the
111 increased exocytosis of AQP2 from recycling endosomes.(6) These studies collectively
112 suggest that VIP17/MAL overexpression results in an imbalance between apical
113 membrane formation and internalization.

114 It is unclear why VIP17/MAL transgenic mice develop renal cystic disease.
115 However, it is well-established that renal cystogenesis occurs in association with defects
116 of the primary cilium, a specialized compartment of the apical membrane with a protein
117 and phospholipid composition that is distinct from that of the remainder of the apical
118 membrane.(44) A number of genetic diseases are attributable to mutations in the genes
119 encoding proteins involved in cilia function. Many of these "ciliopathies" include among
120 their rosters of characteristic symptoms the presence of renal cysts. (29, 38, 48, 52, 56,
121 57, 59) We wondered, therefore, whether the cystic phenotype observed in VIP17/MAL
122 overexpressing mice might be attributable to possible effects of this overexpression on
123 the formation or function of primary cilia.

124 To explore the role of VIP17/MAL in renal cystogenesis and ciliogenesis, we
125 examined the morphology and polarization of wild-type and VIP17/MAL overexpressing
126 MDCK cells grown in two-dimensional and three-dimensional culture. In addition, we
127 evaluated the cilia in both wild-type and VIP17/MAL overexpressing MDCK cells. Our
128 *in vitro* and *in vivo* studies demonstrate that both epithelial morphogenesis and ciliary
129 structure are profoundly perturbed in cells that overexpress VIP17/MAL. These

130 observations suggest an explanation for the renal cystic phenotype observed in
131 VIP17/MAL transgenic mice.
132

133 **MATERIALS AND METHODS:**
134
135 *Cell Culture, Cell Lines, and Transfection*

136 MDCK type II cells were cultured in α-MEM (GIBCO) supplemented with 10%
137 fetal bovine serum, 2mM L-glutamine, 50U/ml penicillin, and 50 ug/ml streptomycin, in
138 a humidified incubator with 5% CO_2. VIP17/MAL overexpressing MDCK cells were
139 similarly cultured. Three independent clones of VIP17/MAL overexpressing MDCK
140 cells were generated and examined for these studies.

141 The coding sequence for VIP17/MAL (NM_005434.4) was inserted into
142 pcDNA^{TM} 3.1^{+} vector (Invitrogen, Carlsbad, CA) using Nhe1 and XbaI. A Flag sequence
143 was subsequently inserted at the amino-terminus by PCR amplification using the primers
144 F-5′-
145 GCCCAAGCTTATG**GACTACAAGGACGACGATGACAAG**GCCCCCGCAGCGG
146 CGACGGGG-3′ (Flag epitope in bold, HindIII site underlined) and R-5′-
147 GCGCCTCGAGTTATGAAGACTTCCATCTGAT-3′ (KpnI site underlined) and
148 subcloned as previously described.(23)

149 MDCK cells were stably transfected with Lipofectamine 2000 (Invitrogen).
150 Clones were selected by growth in medium supplemented with 1.6 mg/mL Zeomycin and
151 screened by immunofluorescence.
152

153 *In vitro cystogenesis*

154 Briefly, 1 x 10^5 MDCK or VIP17/MAL overexpressing cells were suspended in
155 Matrigel (BD Biosciences, Inc.) per the protocol previously described by Grantham et
156 al.(31) All suspensions were co-incubated with MDCK culture medium as described

157 above, with media being replaced every other day. Matrigel suspensions were then
158 placed at 95º Celsius until melted, at which point the cysts were allowed to settle to the
159 bottom of the well for image capture by light microscopy. For cyst immunofluorescence,
160 cysts were retained within the gel.
161
162 *Immunofluorescence in two-dimensions and three-dimensions*
163 Cells on coverslips were washed twice with cold PBS (Sigma-Aldrich) with 1mM
164 $MgCl_2$ and 100 μM $CaCl_2$ (PBS^{2+}) and fixed for 30 minutes in 4% PFA at room
165 temperature. Cells were subsequently washed with PBS^{2+} and then permeabilized with
166 permeabilization buffer (0.3% Triton X-100/0.1% BSA in PBS). Cells were incubated
167 for 1 hour with anti-acetylated alpha tubulin (Sigma) followed by incubation with
168 fluorescein isothiocyanate- or rhodamine-conjugated anti-rat IgG (Molecular Probes).
169 Nuclei were stained with propidium iodide when required. Cells were visualized on a
170 Zeiss LSM 780 confocal microscope.
171 Immunofluorescence on three-dimensional cysts was performed as previously
172 described by O'Brien et al.(37) Briefly cysts were fixed with 4% PFA for 30 minutes,
173 permeabilized in 0.025% saponin for 30 minutes, quenched for 10 min with 7mM
174 NH4Cl, 20mM glycine, in PBS^{2+} (pH8) and then incubated overnight with primary
175 antibody to anti-ZO-1 (Chemicon), anti-E-cadherin (Sigma), anti-β-catenin (Sigma), anti-
176 FLAG (Sigma), anti-gp58 (gift of Ira Mellman) or anti-gp135 (gift of Ira Mellman) as
177 indicated, diluted in goat serum. Cysts were washed for 2-4 hours with saponin in PBS^{2+}
178 and incubated with secondary antibodies overnight. All other details of three-
179 dimensional immunofluorescence are the same as those outlined in the protocol for

180 immunofluorescence analysis of cells grown in two-dimensions that is described above.
181 Cells were visualized using confocal microscopy (Zeiss LSM 780) at 40x and 63x.
182 Images were processed using LSM Image Viewer (Carl Zeiss, Inc.)
183
184 *Quantitative RT-PCR.*
185 RNA from WT and VIP17-overexpressing MDCK cells was purified using the RNeasy
186 kit (Qiagen, Germany). cDNA was synthesized using Superscript III Reverse
187 Transcriptase (Invitrogen) according to the manufacturer's instructions. Quantitative RT-
188 PCR was performed using the QuantiTect SYBR Green PCR kit (Qiagen). Initial
189 denaturation was performed for 10 min at 95°C, and amplification was performed for 40
190 cycles, at 95°C for 30 s, 57°C for 1 min, and 72°C for 1 min. To amplify exogenous
191 human VIP17, the primers 5'-GTACATAATTGGAGCCCACGGTGGA-3′ (sense) and
192 5'-AAGCCGTCTTGCATCGTGATGGT-3′ (antisense) were used, resulting in a 135-bp
193 product. To amplify endogenous canine VIP17, the primers 5'-
194 CACCACAGCCCTGCTTGTCCTGT-3′ (sense) and 5'-
195 TCCCAATGGTGGCCAAAGCTTCC-3′ (antisense) were used, resulting in a 143-bp
196 product. The products were confirmed by agarose gel electrophoresis, and quantified
197 using the $\Delta\Delta C_T$ method with β-actin as a reference gene. VIP17 expression in WT
198 MDCK cells was normalized to 1.
199
200 *Immunohistochemistry*
201 Both wild-type and VIP-17/MAL transgenic mouse kidneys were fixed in 4%
202 paraformaldehyde before being immersed in 30% sucrose and then embedded in

203 OCT.(19) Cryosections (5 μM) were obtained, and sections were then processed for
204 immunofluorescence experiments. Briefly, sections were washed three times in TBS, and
205 then incubated for 5 minutes in TBS with 1% SDS before being washed in TBS again.
206 Following blocking in Goat Serum Dilution Buffer (GSDB; 10% goat serum, 1% Triton
207 X-100, and 10 mM glycine in PBS supplemented with 100 μM $CaCl_2$ and 1 mM $MgCl_2$
208 (PBS^{++})), sections were incubated with a rabbit polyclonal antibody to ADP-ribosylation
209 factor-like protein 13B (ARL13B) (7) (kind gift of Dr. S. Weatherbee, Yale University,
210 used at 1:1,000) and a mouse monoclonal antibody to Na,K-ATPase (41) (Millipore, used
211 at 1:400) diluted in GSDB. Sections were then washed again in TBS before being
212 incubated with an anti-rabbit rhodamine and anti-mouse FITC secondary antibody (also
213 diluted in GSDB) for 1 hour at room temperature. After a final set of washes in TBS,
214 sections were examined and pictures were taken using a Leica confocal microscope.
215 Ciliary length was quantitated using NIS Elements Imaging Software (Nikon).
216 Only unfolded cilia were used for quantitation, with 3 cilia measured per mouse from 3
217 control and 3 VIP17/MAL transgenic mice for a total n of 9 per condition.
218
219 *Statistical Analysis*
220 We calculated the statistical significance of differences in results using unpaired
221 Student's t-tests. We considered a p-value less than 0.05 to be statistically significant.
222

223 **RESULTS:**

224 *VIP17/MAL overexpressing MDCK cells display apical localization of VIP17/MAL.*

225 To investigate the role of VIP17/MAL in epithelial polarization and cyst
226 formation, we used Madin Darby canine kidney (MDCK) cells, a model system
227 extensively employed for *in vitro* studies of epithelial membrane polarization. These
228 cultured renal epithelial cells were stably transfected with a cDNA encoding the
229 VIP17/MAL protein tagged with a FLAG epitope at its amino terminus. Three
230 independent clones of VIP/MAL overexpressing MDCK cells were examined.
231 Quantitative PCR using primers sets designed to detect expression of either the
232 endogenous canine VIP17/MAL transcript or the transcript produce from the transfected
233 human VIP/17 MAL construct indicated that the transfected cells express ~175 fold
234 higher levels of VIP17/MAL mRNA than do untransfected cells. To determine the sub-
235 cellular localization of the VIP17/MAL protein, we performed immunofluorescence
236 studies on fully differentiated and intact monolayers of MDCK cells (**Figure 1a**). Using
237 an antibody directed against the FLAG-epitope, we observed that the VIP17/MAL
238 protein is present primarily on the apical membranes of MDCK cells, consistent with
239 prior reports.(9, 61) Interestingly, the VIP17/MAL protein was detected over the entire
240 apical surface and was apparently able to access the "exclusion zones" that surround the
241 bases of cilia.(17) Consistent with this observation, the overexpressed VIP17/MAL
242 protein could also be detected in a punctate distribution in some but not all cilia (**Figure**
243 **1c**). Western blot analysis of protein extracts prepared from these cells (**Figure 1b**) using
244 both monoclonal and polyclonal anti-FLAG antibodies detects a protein with the
245 anticipated size of 17kD.

246

247 *VIP17/MAL overexpressing cysts have altered morphology.*

248 The presence of amplified apical membranes in VIP17/MAL overexpressing
249 MDCK cells grown in two-dimensional culture suggests that VIP17/MAL plays a role in
250 regulating vesicular traffic to and from the apical membrane.(9, 42, 61) To evaluate the
251 effect of VIP17/MAL on epithelial morphogenesis, VIP17/MAL overexpressing MDCK
252 cells and wild-type MDCK cells were suspended in a three-dimensional collagen matrix
253 and allowed to form cysts spontaneously as previously described.(31) While
254 untransfected MDCK cells generally formed cysts surrounding a single lumen, cysts
255 produced by VIP17/MAL overexpressing cells were significantly more likely to exhibit
256 multiple lumens (**Figure 2a**). The difference in lumen number is quantified in **Figure 2b**
257 ($p<0.01$). Both proliferative rate and the level of the mTOR activity have been shown to
258 be elevated in the context of renal cystic disease (8, 51), so we assessed the proliferation
259 rate and mTOR activity in VIP17/MAL overexpressing MDCK cells by
260 immunofluorescence staining for Ki67 and western blotting for phospho-S6 kinase,
261 respectively. This analysis revealed no differences between the wild type and
262 VIP17/MAL overexpressing cells (not shown). It is interesting and perhaps somewhat
263 surprising to note that a similar multiple lumen phenotype is observed with MDCK cells
264 in which VIP17/MAL expression has been reduced through treatment with RNAi.(53)
265 While the mechanisms responsible for multiple lumen formation in the context of
266 VIP17/MAL knockdown and overpression may not be identical, together these results
267 suggest that a specific level of VIP17/MAL expression is required in order to drive the

268 cavitation process responsible for MDCK cyst lumen formation towards the production
269 of a single central lumen.
270
271 *E-cadherin, β-catenin, gp58 and ZO-1expression in VIP17/MAL overexpressing cysts is*
272 *similar to that of control MDCK cysts.*
273 The multiple lumen formation that we observed in VIP17/MAL overexpressing
274 cell cysts could, in principle, arise as a consequence of a defect in the function of
275 membrane protein polarity or sorting pathways. To assess this possibility, we examined
276 the distribution and expression of several markers of epithelial polarity. E-cadherin is a
277 calcium-dependent cell adhesion molecule, which binds to a catenin protein complex (α
278 and β) to mediate cell-cell adhesion, and polarized epithelium formation.(54, 58)
279 Polycystin-1, one of two proteins implicated in ADPKD, interacts with the E-cadherin
280 complex containing β-catenin, and a large body of evidence suggests that aberrant β-
281 catenin mediated Wnt signaling may be involved in cystogenesis.(4, 22, 27, 43, 45, 46,
282 50)
283 To test whether the localization of E-cadherin and β-catenin is disrupted in
284 VIP17/MAL overexpressing cell cysts, immunofluorescence studies were performed, and
285 protein localization was evaluated by laser scanning confocal microscopy. There is
286 normal basolateral localization of E-cadherin in both WT (**Figure 3a**) and VIP17/MAL
287 overexpressing cell cysts (**Figure 4a**). Under normal circumstances, β-catenin localizes
288 to the perinuclear cytoplasm or to the basolateral membrane, where it engages with E-
289 cadherin.(26) In cysts formed from wild-type MDCK cells (**Figure 3b**) or VIP17/MAL
290 overexpressing cells (**Figure 4b**), β-catenin retains its classic distribution along the

291 basolateral membrane. Finally, immunofluorescence was used to assess the distribution
292 of the basolateral marker antigen identified as gp58, which is the β-subunit of the Na,K-
293 ATPase. This protein also retains a basolateral distribution independent of VIP17/MAL
294 overexpression (**Figures 3c, 4c**). (3, 20) We conclude that VIP17/MAL overexpression
295 does not affect the distribution of E-cadherin, β-catenin, or gp58 in an *in vitro* model of
296 cystogenesis.

297 Zona occludens 1 (ZO-1) is a classic structural component of tight junctions in
298 MDCK cells.(2) The integrity of the tight junction is important for establishing the
299 extent and nature of the paracellular ion permeability barrier, which in turn plays a role in
300 the mechanisms responsible for luminal fluid secretion.(13, 60) We therefore examined
301 the localization of ZO-1 in cysts composed of wild-type MDCK cells or VIP17/MAL
302 overexpressing MDCK cells. By immunofluorescence and confocal imaging, ZO-1 was
303 abundantly expressed and properly localized to tight junctions in both cyst types (data not
304 shown). We conclude that VIP17/MAL expression does not have an obvious effect on
305 ZO-1 localization.

306

307 *VIP17/MAL overexpression results in apical accumulation of gp135 with aberrant*
308 *localization of this protein to the primary cilium.*

309 Gp135, also known as podocalyxin, is endogenously expressed and localized to
310 the apical membrane in MDCK cells.(33) VIP17/MAL overexpression results in
311 increased apical expression of the influenza virus hemagglutinin, among other proteins
312 (9). In VIP17/MAL overexpressing MDCK cysts, immunofluorescence localization of
313 gp135 reveals a surprising alteration in this protein's distribution. In control MDCK

314 cells, gp135 is not present in the cilium that extends from the apical surface, accounting
315 for the characteristic pattern of "ciliary exclusion" that is observed when the pattern of
316 gp135 localization is observed in the apical surfaces of MDCK cells viewed en face.(17)
317 Interestingly, it appears that gp135 localizes to the primary cilium in VIP17/MAL over-
318 expressing MDCK cells grown in three-dimensional cyst culture (**Figure 5a**). This
319 behavior was also detected in two-dimensional cultures, in which we determined that
320 VIP17/MAL overexpression correlates with ciliary localization of gp135 (**Figure 5b**).
321 Gp135 is notably absent from the cilia of control MDCK cells grown either under two or
322 three dimensional culture conditions (**Figure 5a and b**).
323
324 *VIP17/MAL overexpression results in shortened or absent cilia* in vitro *and* in vivo.
325 Since VIP17/MAL transgenic mice are reported to develop renal cysts, and
326 susceptibility to the formation of renal cysts is frequently associated with perturbations
327 that produce ciliary defects, we next examined the cilia of MDCK cysts grown *in vitro*.
328 Untransfected MDCK cells and VIP17/MAL overexpressing MDCK cells were both
329 suspended in a collagenous matrix, and immunofluorescence analysis, employing an
330 antibody directed against acetylated tubulin, was used to visualize the ciliary axoneme.
331 As shown in **Figure 6**, we found that MDCK cell cysts demonstrated long cilia that
332 extended well into the lumen, consistent with our previous observations and those of
333 others.(55) In contrast, cysts produced by VIP17/MAL overexpressing cells displayed
334 stunted or absent cilia. Moreover, even when present, primary cilia did not appear to be
335 protruding extensively into the lumen. Therefore, we conclude that VIP17/MAL

336 overexpression perturbs cilia formation, extension or stability in a model of renal
337 epithelial cells grown in 3D culture *in vitro*.

338 We also evaluated the primary cilia of kidneys isolated from transgenic
339 VIP17/MAL overexpressing mice (**Figure 7**). Immunofluorescence analysis was
340 performed on the kidneys of adult mice using an anti-ARL13B antibody (7) to label the
341 cilium and an anti-Na,K-ATPase antibody (41) to identify the basolateral membrane.
342 ARL13B is the ciliary protein mutated in Joubert syndrome (5). In parallel with our *in*
343 *vitro* findings, we readily observed the presence of long, protruding cilia within the
344 lumina of the renal tubules of wild type control mice of the same genetic strain. In
345 contrast, cilia were significantly stunted or absent in the dilated lumina/cysts of the renal
346 tubules of in tissue from a VIP17/MAL overexpressing transgenic mouse model. The
347 average lengths of these cilia were roughly half of those measured in similar renal tubule
348 segments of wild type animals (6 μM versus 12 μM, $p<0.01$). These studies suggest that
349 VIP17/MAL overexpression results in the development of abnormal cilia.

350

351

352 **DISCUSSION:**

353 We find that VIP17/MAL overexpression results in abnormal cilia and cyst
354 development in renal epithelial cells, *in vitro* and *in vivo*. In the well-studied MDCK cell
355 culture model of *in vitro* epithelial cystogenesis, VIP17/MAL overexpressing cells
356 formed multi-lumen cysts more frequently than did control cells, and their cilia were
357 either shortened or absent. The VIP17/MAL transgenic mice are known to develop renal
358 cysts (18), and we show that the cilia in these structures are also diminished in number
359 and size as compared to those found in association with the epithelial cells of renal
360 tubules from wild type animals. These phenotypes are present in the context of normal
361 sorting of basolateral membrane proteins, including E-cadherin, β-catenin, the Na,K-
362 ATPase and ZO-1. In contrast, the distribution of the apical marker protein gp135 is
363 markedly abnormal in the VIP/MAL over-expressing cells. The presence of this
364 polypeptide on the apical surface appears to be increased and, most importantly, it is no
365 longer excluded from the cilium in the VIP17/MAL over-expressing cells. This
366 observation suggests that over-expression of VIP17/MAL perturbs the formation or
367 maintenance of the barrier that normally maintains the unique composition of the ciliary
368 membrane by preventing intermixing of apical and ciliary membrane components.(30)

369 VIP17/MAL has been proposed to facilitate the apical delivery of several newly
370 synthesized membrane proteins, including influenza hemagglutinin, gp80, and gp114.(9,
371 42) This function is supported by *in vitro* studies in which decreased levels of
372 VIP17/MAL result in aberrant trafficking of these apical proteins to the basolateral
373 membrane in MDCK monolayers. In contrast, overexpression of VIP17/MAL in this
374 same cultured epithelial model system leads to expansion of the apical plasma membrane

375 surface area, suggesting increased delivery or decreased retrieval of apical
376 components.(9, 42, 61)

377 VIP17/MAL has been shown to decrease the rate of endocytosis of the aquaporin-
378 2 water channel and thus to stabilize its residence in the apical plasma membrane.(23) It
379 is therefore possible that an imbalance in the rates of endocytosis and exocytosis is
380 responsible for the capacity of VIP17/MAL overexpression to induce the development of
381 amplified renal epithelial cell membranes.(18) In contrast to the flattened cyst lining
382 epithelia observed in the most common renal cystic disease, ADPKD, the cells lining the
383 cysts of VIP17/MAL overexpressing mice exhibit ballooning or blebbing of the apical
384 membrane into the cyst lumen, with a pseudostratified morphology.(18) Collectively,
385 these data support the premise that VIP17/MAL may contribute to cystogenesis through
386 perturbations in the structure of the apical membrane induced by disrupting the strict
387 balance between endocytosis and exocytosis that normally determines the surface area of
388 the apical plasma membrane domain.

389 In genetic polycystic kidney diseases, including autosomal dominant polycystic
390 kidney disease, autosomal recessive polycystic kidney disease, and the nephronopthises,
391 the proteins encoded by the responsible genes are often localized to the primary
392 cilium.(49) Renal cysts are therefore common features of the "ciliopathies", the family
393 of genetic diseases attributable to perturbations on genes whose protein products
394 contribute to ciliary structure or function. The common mechanism underlying these
395 diseases involves disruption of the primary cilium or proteins that co-localize with it.(39)
396 The primary cilium is formed when the designated mother centriole is modified to
397 assume its role as the basal body beneath the cell's apical surface.(40) Ciliogenesis

398 ensues, with the cell directing necessary cargo to the tip of the cilium in a process known
399 as intraflagellar transport.

400 Ciliopathies can result from either abnormal transport of proteins within the
401 cilium or from disrupted delivery of vesicles from intracellular compartments to the base
402 of the cilium. (10, 16) Recent data suggests that while targeting of ciliary proteins to the
403 cilium may occur via lateral transport from within the cell's apical membrane (34), there
404 is also a component of targeted exocytosis to the base of the cilium.(15) This cargo
405 navigates through or across the peri-ciliary membrane or ciliary necklace and is
406 subsequently trafficked into the cilium.(28) While VIP17/MAL has not previously been
407 implicated in ciliary trafficking, a number of other proteins similarly implicated in
408 epithelial polarity have been shown to be involved in ciliogenesis.(11, 12, 14, 62) It is
409 also worth noting that recent studies have shown that Septin 2, a guanosine
410 triphosphatase is located at the base of the ciliary membrane and is thought to be part of a
411 diffusion barrier that maintains the unique composition of the ciliary membrane.(21)
412 When Septin 2 is absent, the structure of the ciliary membrane is destroyed and abnormal
413 or abrogated ciliary growth occurs.

414 When VIP17/MAL was overexpressed in cultured MDCK cells *in vitro*, we noted
415 that cilia were also shortened and compositionally altered, with aberrant sorting of gp135
416 to the cilium. These observations suggest the interesting interpretation that the barrier
417 regulating ciliary protein trafficking had been disrupted. According to this model,
418 VIP17/MAL overexpression may either perturb the sorting of those proteins to the cilium
419 that are required for maintaining the ciliary barrier, or VIP17/MAL may itself directly
420 disturb this boundary. Regardless, given this disturbance, it is perhaps expected that

421 ciliary structure and thereby function is altered, leading to shortened and developmentally
422 altered cilia, such as those seen in Figures 6, and to an *in vivo* phenotype that bears the
423 hallmarks of a ciliopathy (Figure 7). It is important to note that our analysis of ciliary
424 length in wild type and VIP17/MAL overexpressing kidneys was limited to a relatively
425 small number of specimens, and thus the results need to be interpreted with caution.
426 Nevertheless, our data suggest the novel possibility that VIP17/MAL overexpression
427 produces renal cysts *in vivo* by inducing the production of over-abundant apical
428 membrane, which in turn disrupts the composition and structure of the cilium. Thus, the
429 cysts observed in VIP17/MAL overexpression may be seen as arising as the consequence
430 of a "secondary ciliopathy."

431 These studies highlight the relationship between epithelial cell polarization and
432 ciliogenesis, which results in cystogenesis when disrupted. VIP17/MAL appears to be a
433 central component involved in both of these processes. When evaluated collectively,
434 these data suggest a connection between cilia formation, post-Golgi sorting mechanisms,
435 and epithelial cell polarization in renal cystogenesis.

436

437

GRANTS:

This work was supported by NIH MSTP TG 5T32GM07205 and F30DK083221 to VT and NIH DK57328 and DK17433 to MJC. These studies made use of imaging resources provided through the Center for Polycystic Kidney disease Research at Yale (NIH DK090744)

AUTHOR CONTRIBUTIONS:

V.T. designed and performed the experiments and wrote the manuscript. K.M. and M.C. assisted with and helped to analyze the *in vitro* and *ex vivo* experiments, respectively. N.S-W. developed the VIP17/MAL overexpressing mouse model. MJC directed the project and assisted with manuscript preparation.

DISCLOSURES:

The authors of this manuscript have no conflicts of interests or disclosures.

455 **REFERENCES:**
456
457
458
459

460 1. **Alonso MA, and Weissman SM**. cDNA cloning and sequence of MAL, a
461 hydrophobic protein associated with human T-cell differentiation. *Proc Natl Acad Sci U*
462 *S A* 84: 1997-2001, 1987.

463 2. **Anderson JM, Stevenson BR, Jesaitis LA, Goodenough DA, and Mooseker**
464 **MS**. Characterization of ZO-1, a protein component of the tight junction from mouse
465 liver and Madin-Darby canine kidney cells. *J Cell Biol* 106: 1141-1149, 1988.

466 3. **Balcarova-Stander J, Pfeiffer SE, Fuller SD, and Simons K**. Development of
467 cell surface polarity in the epithelial Madin-Darby canine kidney (MDCK) cell line.
468 *Embo J* 3: 2687-2694, 1984.

469 4. **Boca M, D'Amato L, Distefano G, Polishchuk RS, Germino GG, and Boletta**
470 **A**. Polycystin-1 induces cell migration by regulating phosphatidylinositol 3-kinase-
471 dependent cytoskeletal rearrangements and GSK3beta-dependent cell cell mechanical
472 adhesion. *Mol Biol Cell* 18: 4050-4061, 2007.

473 5. **Cantagrel V, Silhavy JL, Bielas SL, Swistun D, Marsh SE, Bertrand JY,**
474 **Audollent S, Attie-Bitach T, Holden KR, Dobyns WB, Traver D, Al-Gazali L, Ali**
475 **BR, Lindner TH, Caspary T, Otto EA, Hildebrandt F, Glass IA, Logan CV,**
476 **Johnson CA, Bennett C, Brancati F, Valente EM, Woods CG, and Gleeson JG**.
477 Mutations in the cilia gene ARL13B lead to the classical form of Joubert syndrome. *Am J*
478 *Hum Genet* 83: 170-179, 2008.

479 6. **Carmosino M, Rizzo F, Procino G, Basco D, Valenti G, Forbush B, Schaeren-**
480 **Wiemers N, Caplan MJ, and Svelto M**. MAL/VIP17, a new player in the regulation of
481 NKCC2 in the kidney. *Mol Biol Cell* 21: 3985-3997.

482 7. **Caspary T, Larkins CE, and Anderson KV**. The graded response to Sonic
483 Hedgehog depends on cilia architecture. *Dev Cell* 12: 767-778, 2007.

484 8. **Chapin HC, and Caplan MJ**. The cell biology of polycystic kidney disease. *J*
485 *Cell Biol* 191: 701-710, 2010.

486 9. **Cheong KH, Zacchetti D, Schneeberger EE, and Simons K**. VIP17/MAL, a
487 lipid raft-associated protein, is involved in apical transport in MDCK cells. *Proc Natl*
488 *Acad Sci U S A* 96: 6241-6248, 1999.

489 10. **Dentler W**. Intraflagellar transport (IFT) during assembly and disassembly of
490 Chlamydomonas flagella. *J Cell Biol* 170: 649-659, 2005.

491 11. **Fan S, Fogg V, Wang Q, Chen XW, Liu CJ, and Margolis B**. A novel
492 Crumbs3 isoform regulates cell division and ciliogenesis via importin beta interactions. *J*
493 *Cell Biol* 178: 387-398, 2007.

494 12. **Fan S, Hurd TW, Liu CJ, Straight SW, Weimbs T, Hurd EA, Domino SE,**
495 **and Margolis B**. Polarity proteins control ciliogenesis via kinesin motor interactions.
496 *Curr Biol* 14: 1451-1461, 2004.

497 13. **Fanning AS, Mitic LL, and Anderson JM**. Transmembrane proteins in the tight
498 junction barrier. *J Am Soc Nephrol* 10: 1337-1345, 1999.

499 14. **Fogelgren B, Lin SY, Zuo X, Jaffe KM, Park KM, Reichert RJ, Bell PD,**
500 **Burdine RD, and Lipschutz JH**. The Exocyst Protein Sec10 Interacts with Polycystin-2
501 and Knockdown Causes PKD-Phenotypes. *PLoS Genet* 7: e1001361.

502 15. **Follit JA, Li L, Vucica Y, and Pazour GJ**. The cytoplasmic tail of fibrocystin
503 contains a ciliary targeting sequence. *J Cell Biol* 188: 21-28.

504 16. **Follit JA, Tuft RA, Fogarty KE, and Pazour GJ**. The intraflagellar transport
505 protein IFT20 is associated with the Golgi complex and is required for cilia assembly.
506 *Mol Biol Cell* 17: 3781-3792, 2006.

507 17. **Francis SS, Sfakianos J, Lo B, and Mellman I**. A hierarchy of signals regulates
508 entry of membrane proteins into the ciliary membrane domain in epithelial cells. *J Cell*
509 *Biol* 193: 219-233.

510 18. **Frank M, Atanasoski S, Sancho S, Magyar JP, Rulicke T, Schwab ME, and**
511 **Suter U**. Progressive segregation of unmyelinated axons in peripheral nerves, myelin
512 alterations in the CNS, and cyst formation in the kidneys of myelin and lymphocyte
513 protein-overexpressing mice. *J Neurochem* 75: 1927-1939, 2000.

514 19. **Frank M, van der Haar ME, Schaeren-Wiemers N, and Schwab ME**. rMAL
515 is a glycosphingolipid-associated protein of myelin and apical membranes of epithelial
516 cells in kidney and stomach. *J Neurosci* 18: 4901-4913, 1998.

517 20. **Fullekrug J, Shevchenko A, and Simons K**. Identification of glycosylated
518 marker proteins of epithelial polarity in MDCK cells by homology driven proteomics.
519 *BMC Biochem* 7: 8, 2006.

520 21. **Hu Q, Milenkovic L, Jin H, Scott MP, Nachury MV, Spiliotis ET, and Nelson**
521 **WJ**. A septin diffusion barrier at the base of the primary cilium maintains ciliary
522 membrane protein distribution. *Science* 329: 436-439.

523 22. **Huan Y, and van Adelsberg J**. Polycystin-1, the PKD1 gene product, is in a
524 complex containing E-cadherin and the catenins. *J Clin Invest* 104: 1459-1468, 1999.

525 23. **Kamsteeg EJ, Duffield AS, Konings IB, Spencer J, Pagel P, Deen PM, and**
526 **Caplan MJ**. MAL decreases the internalization of the aquaporin-2 water channel. *Proc*
527 *Natl Acad Sci U S A* 104: 16696-16701, 2007.

528 24. **Kang DY, Park JI, Cho WS, Jeong MH, Cho GW, Park HT, and Bae HR**.
529 Identification of vasopressin-induced genes in AQP2-transfected MDCK cells by
530 suppression subtractive hybridization. *Biochem Biophys Res Commun* 324: 1234-1241,
531 2004.

532 25. **Kim T, Fiedler K, Madison DL, Krueger WH, and Pfeiffer SE**. Cloning and
533 characterization of MVP17: a developmentally regulated myelin protein in
534 oligodendrocytes. *J Neurosci Res* 42: 413-422, 1995.

535 26. **Kugoh H, Kleymenova E, and Walker CL**. Retention of membrane-localized
536 beta-catenin in cells lacking functional polycystin-1 and tuberin. *Mol Carcinog* 33: 131-
537 136, 2002.

538 27. **Lal M, Song X, Pluznick JL, Di Giovanni V, Merrick DM, Rosenblum ND,**
539 **Chauvet V, Gottardi CJ, Pei Y, and Caplan MJ**. Polycystin-1 C-terminal tail
540 associates with beta-catenin and inhibits canonical Wnt signaling. *Hum Mol Genet* 17:
541 3105-3117, 2008.

542 28. **Lim YS, Chua CE, and Tang BL**. Rabs and other small GTPases in ciliary
543 transport. *Biol Cell* 103: 209-221.

544 29. **Lin F, Hiesberger T, Cordes K, Sinclair AM, Goldstein LS, Somlo S, and**
545 **Igarashi P**. Kidney-specific inactivation of the KIF3A subunit of kinesin-II inhibits renal
546 ciliogenesis and produces polycystic kidney disease. *Proc Natl Acad Sci U S A* 100:
547 5286-5291, 2003.

548 30. **Magal LG, Yaffe Y, Shepshelovich J, Aranda JF, de Marco Mdel C, Gaus K,**
549 **Alonso MA, and Hirschberg K**. Clustering and lateral concentration of raft lipids by the
550 MAL protein. *Mol Biol Cell* 20: 3751-3762, 2009.

551 31. **Mangoo-Karim R, Uchic M, Lechene C, and Grantham JJ**. Renal epithelial
552 cyst formation and enlargement in vitro: dependence on cAMP. *Proc Natl Acad Sci U S A*
553 86: 6007-6011, 1989.

554 32. **Martin-Belmonte F, Kremer L, Albar JP, Marazuela M, and Alonso MA**.
555 Expression of the MAL gene in the thyroid: the MAL proteolipid, a component of
556 glycolipid-enriched membranes, is apically distributed in thyroid follicles. *Endocrinology*
557 139: 2077-2084, 1998.

558 33. **Meder D, Shevchenko A, Simons K, and Fullekrug J**. Gp135/podocalyxin and
559 NHERF-2 participate in the formation of a preapical domain during polarization of
560 MDCK cells. *J Cell Biol* 168: 303-313, 2005.

561 34. **Milenkovic L, Scott MP, and Rohatgi R**. Lateral transport of Smoothened from
562 the plasma membrane to the membrane of the cilium. *J Cell Biol* 187: 365-374, 2009.

563 35. **Millan J, and Alonso MA**. MAL, a novel integral membrane protein of human T
564 lymphocytes, associates with glycosylphosphatidylinositol-anchored proteins and Src-
565 like tyrosine kinases. *Eur J Immunol* 28: 3675-3684, 1998.

566 36. **Millan J, Puertollano R, Fan L, and Alonso MA**. Caveolin and MAL, two
567 protein components of internal detergent-insoluble membranes, are in distinct lipid
568 microenvironments in MDCK cells. *Biochem Biophys Res Commun* 233: 707-712, 1997.

569 37. **O'Brien LE, Jou TS, Pollack AL, Zhang Q, Hansen SH, Yurchenco P, and**
570 **Mostov KE**. Rac1 orientates epithelial apical polarity through effects on basolateral
571 laminin assembly. *Nat Cell Biol* 3: 831-838, 2001.

572 38. **Ong AC, and Wheatley DN**. Polycystic kidney disease--the ciliary connection.
573 *Lancet* 361: 774-776, 2003.

574 39. **Pazour GJ, and Rosenbaum JL**. Intraflagellar transport and cilia-dependent
575 diseases. *Trends Cell Biol* 12: 551-555, 2002.

576 40. **Pearson CG, Culver BP, and Winey M**. Centrioles want to move out and make
577 cilia. *Dev Cell* 13: 319-321, 2007.

578 41. **Pietrini G, Matteoli M, Banker G, and Caplan MJ**. Isoforms of the Na,K-
579 ATPase are present in both axons and dendrites of hippocampal neurons in culture. *Proc*
580 *Natl Acad Sci U S A* 89: 8414-8418., 1992.

581 42. **Puertollano R, Martin-Belmonte F, Millan J, de Marco MC, Albar JP,**
582 **Kremer L, and Alonso MA**. The MAL proteolipid is necessary for normal apical
583 transport and accurate sorting of the influenza virus hemagglutinin in Madin-Darby
584 canine kidney cells. *J Cell Biol* 145: 141-151., 1999.

585 43. **Qian CN, Knol J, Igarashi P, Lin F, Zylstra U, Teh BT, and Williams BO**.
586 Cystic renal neoplasia following conditional inactivation of apc in mouse renal tubular
587 epithelium. *J Biol Chem* 280: 3938-3945, 2005.

588 44. **Reiter JF, and Mostov K**. Vesicle transport, cilium formation, and membrane
589 specialization: the origins of a sensory organelle. *Proc Natl Acad Sci U S A* 103: 18383-
590 18384, 2006.

591 45. **Roitbak T, Ward CJ, Harris PC, Bacallao R, Ness SA, and Wandinger-Ness**
592 **A**. A polycystin-1 multiprotein complex is disrupted in polycystic kidney disease cells.
593 *Mol Biol Cell* 15: 1334-1346, 2004.

594 46. **Saadi-Kheddouci S, Berrebi D, Romagnolo B, Cluzeaud F, Peuchmaur M,**
595 **Kahn A, Vandewalle A, and Perret C**. Early development of polycystic kidney disease

596 in transgenic mice expressing an activated mutant of the beta-catenin gene. *Oncogene* 20:
597 5972-5981, 2001.

598 47. **Simons K, and Wandinger-Ness A**. Polarized sorting in epithelia. *Cell* 62: 207-
599 210., 1990.

600 48. **Simons M, Gloy J, Ganner A, Bullerkotte A, Bashkurov M, Kronig C,**
601 **Schermer B, Benzing T, Cabello OA, Jenny A, Mlodzik M, Polok B, Driever W,**
602 **Obara T, and Walz G**. Inversin, the gene product mutated in nephronophthisis type II,
603 functions as a molecular switch between Wnt signaling pathways. *Nat Genet* 37: 537-
604 543, 2005.

605 49. **Singla V, and Reiter JF**. The primary cilium as the cell's antenna: signaling at a
606 sensory organelle. *Science* 313: 629-633, 2006.

607 50. **Sorenson CM**. Nuclear localization of beta-catenin and loss of apical brush
608 border actin in cystic tubules of bcl-2 -/- mice. *Am J Physiol* 276: F210-217, 1999.

609 51. **Takiar V, and Caplan MJ**. Polycystic kidney disease: Pathogenesis and
610 potential therapies. *Biochim Biophys Acta* 2010.

611 52. **Tammachote R, Hommerding CJ, Sinders RM, Miller CA, Czarnecki PG,**
612 **Leightner AC, Salisbury JL, Ward CJ, Torres VE, Gattone VH, 2nd, and Harris**
613 **PC**. Ciliary and centrosomal defects associated with mutation and depletion of the
614 Meckel syndrome genes MKS1 and MKS3. *Hum Mol Genet* 18: 3311-3323, 2009.

615 53. **Torkko JM, Manninen A, Schuck S, and Simons K**. Depletion of apical
616 transport proteins perturbs epithelial cyst formation and ciliogenesis. *J Cell Sci* 121:
617 1193-1203, 2008.

618 54. **van Adelsberg J**. Protein targeting: the molecular basis of vectorial transport in
619 the kidney. *Semin Nephrol* 18: 152-166, 1998.

620 55. **Vieira OV, Gaus K, Verkade P, Fullekrug J, Vaz WL, and Simons K**. FAPP2,
621 cilium formation, and compartmentalization of the apical membrane in polarized Madin-
622 Darby canine kidney (MDCK) cells. *Proc Natl Acad Sci U S A* 103: 18556-18561, 2006.

623 56. **Wang S, Luo Y, Wilson PD, Witman GB, and Zhou J**. The autosomal
624 recessive polycystic kidney disease protein is localized to primary cilia, with
625 concentration in the basal body area. *J Am Soc Nephrol* 15: 592-602, 2004.

626 57. **Watnick T, and Germino G**. From cilia to cyst. *Nat Genet* 34: 355-356, 2003.

627 58. **Yeaman C, Grindstaff KK, and Nelson WJ**. New perspectives on mechanisms
628 involved in generating epithelial cell polarity. *Physiol Rev* 79: 73-98, 1999.

629 59. **Yoder BK, Tousson A, Millican L, Wu JH, Bugg CE, Jr., Schafer JA, and**
630 **Balkovetz DF**. Polaris, a protein disrupted in orpk mutant mice, is required for assembly
631 of renal cilium. *Am J Physiol Renal Physiol* 282: F541-552, 2002.

632 60. **Yu AS, Kanzawa SA, Usorov A, Lantinga-van Leeuwen IS, and Peters DJ**.
633 Tight junction composition is altered in the epithelium of polycystic kidneys. *J Pathol*
634 216: 120-128, 2008.

635 61. **Zacchetti D, Peranen J, Murata M, Fiedler K, and Simons K**. VIP17/MAL, a
636 proteolipid in apical transport vesicles. *FEBS Lett* 377: 465-469, 1995.

637 62. **Zuo X, Fogelgren B, and Lipschutz JH**. The small GTPase Cdc42 is necessary
638 for primary ciliogenesis in renal tubular epithelial cells. *J Biol Chem*.
639
640
641

642 **FIGURE LEGENDS:**
643
644 *Figure 1: Stable VIP17/MAL expression.*

645 a) Immunofluorescence analysis of MDCK cells stably transfected with Flag-
646 VIP17/MAL. The apical localization of VIP17/MAL is revealed with poly-Flag (red) in
647 both *en face* extended depth of focus (bottom panel) and in XZ cross section (top panel)
648 images. b) Western blot analysis of MDCK cell lines stably transfected with
649 VIP17/MAL. A specific band is detected at 17kD. c) VIP17/MAL (green) is detectable in
650 a punctate pattern in some but not all cilia (labeled with anti-acetylated tubulin; red) in
651 transfected MDCK cells.
652
653 *Figure 2: VIP17/MAL overexpression alters morphology of cultured MDCK cysts.*
654 (a) Representative images of WT MDCK (top) and VIP17/MAL overexpressing MDCK
655 (bottom) cysts, acquired by light microscopy, demonstrating more multi-lumen (arrows)
656 cysts produced by cells overexpressing VIP17/MAL. b) Quantitation of microscopic
657 images revealing an increased incidence of multilumen cysts derived from VIP17/MAL
658 overexpressing MDCK cells** $p<0.01$ (n=100 cysts)
659
660 *Figure 3: Localization of basolateral membrane markers in three-dimensional WT*
661 *MDCK cell cysts.*
662 Immunofluorescence analysis of representative wild type MDCK cell cysts demonstrates
663 the localization of (a) E-cadherin, (b) β-catenin, and (c) gp58 (green) at the basolateral
664 membrane. Propidium iodide (blue) was used to label nuclei. Merged color images are
665 depicted in the right hand panel. All scale bars depicted are 20μm.

666

667 *Figure 4: Basolateral membrane marker expression is unchanged by overexpression of*
668 *VIP17/MAL.*

669 Immunofluorescence analysis of representative VIP17/MAL overexpressing MDCK cell
670 cysts with antibodies to the basolateral markers (a) E-cadherin, (b) β-catenin, and (c)
671 gp58 (green) demonstrates normal basolateral localization, similar to that detected in
672 control MDCK cysts. Hoescht staining (blue) was used to label nuclei. Mono-FLAG (red)
673 indicates VIP17/MAL expression. Merged color images are depicted in the right hand
674 panel. All scale bars depicted are 20μm.

675

676 *Figure 5: VIP17/MAL overexpression results in gp135 apical localization and ciliary*
677 *localization in an in vitro cyst culture model.*

678 (a) Representative WT MDCK (top) and VIP17/MAL overexpressing cell cysts (bottom)
679 depicting expression of the apical marker gp135 (red) at the apical membrane (thick
680 arrow) and in the cilium (thin arrow) (alpha-tubulin; green) in cells expressing
681 VIP17/MAL. (b) Gp135 (red) is present in the primary cilia of VIP17/MAL
682 overexpressing MDCK cells grown in 2D (thin arrows, bottom panel), but is notably
683 absent from WT MDCK cilia and from the ciliary exclusion zones in the apical
684 membranes of WT MDCK cells (thin arrows, top panel). Orthogonal images of the
685 individual cilia indicated by the arrow heads are shown in the upper right corners of the
686 top and bottom panels. All scale bars depicted are 10 μM.

687

688 *Figure 6: VIP17/MAL overexpression results in aberrant ciliogenesis in an in vitro three-*
689 *dimensional cyst culture model.*
690 MDCK cells suspended in Matrigel were analyzed by immunofluorescence to localize
691 acetylated tubulin (green). Nuclei are labeled with propidium iodide (red). Prominent
692 cilia are seen protruding into the apical lumen in wild-type MDCK cysts (top), while very
693 few, shortened cilia are seen in VIP17/MAL overexpressing cysts (bottom). Arrows point
694 to multi-lumen cysts.
695
696 *Figure 7: VIP17/MAL transgenic mice have abnormal cilia.*
697 Immunofluorescence analysis to detect cilia in control (CTRL) and VIP17/MAL
698 transgenic mice. Renal sections were labeled with antibody directed against the ciliary
699 protein, Arl13b (red) and the Na,K-ATPase (green). Control mice display readily
700 detectable, long cilia protruding into the distal tubule lumen, while VIP17/MAL
701 transgenic mice display fewer and smaller cilia within their dilated lumina/cysts**.** Scale
702 bars (lower right of both panels) are 10 μM.
703

Figure 1

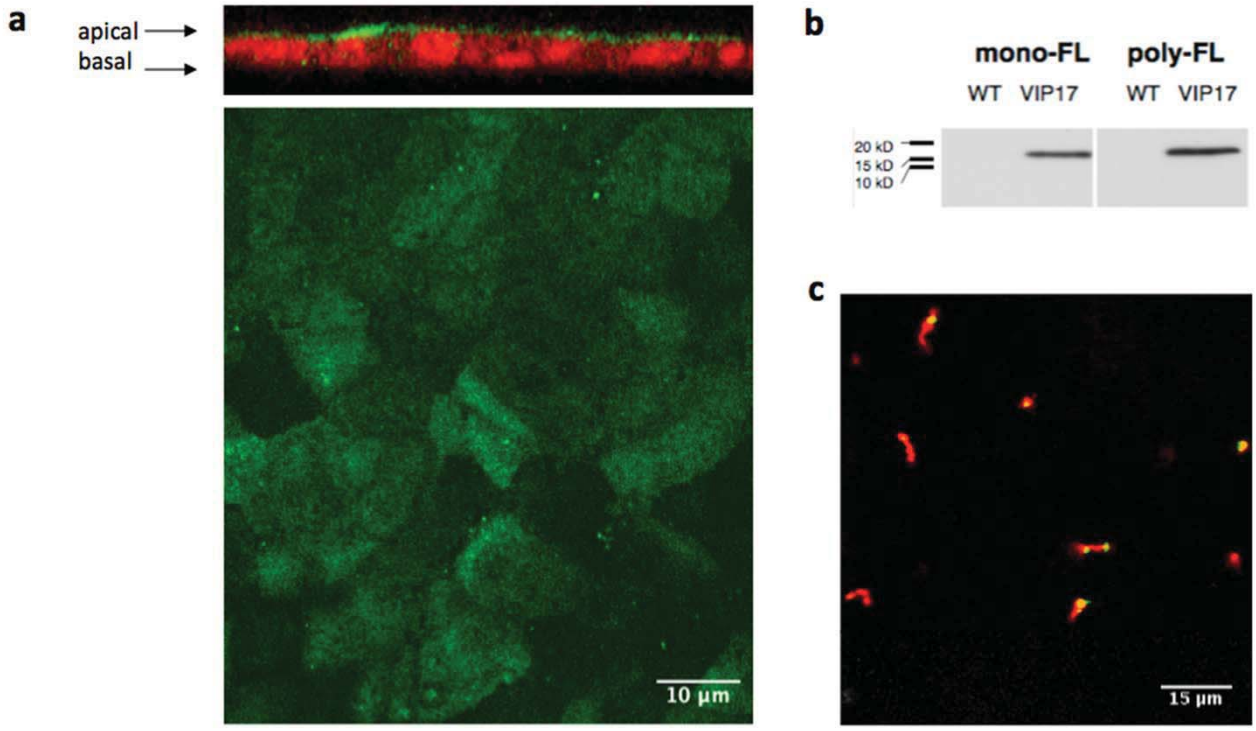
a
apical
basal
10 µm
b
mono-FL
poly-FL
WT
VIP17
WT
VIP17
20 kD
15 kD
10 kD
c
15 µm

Figure 2

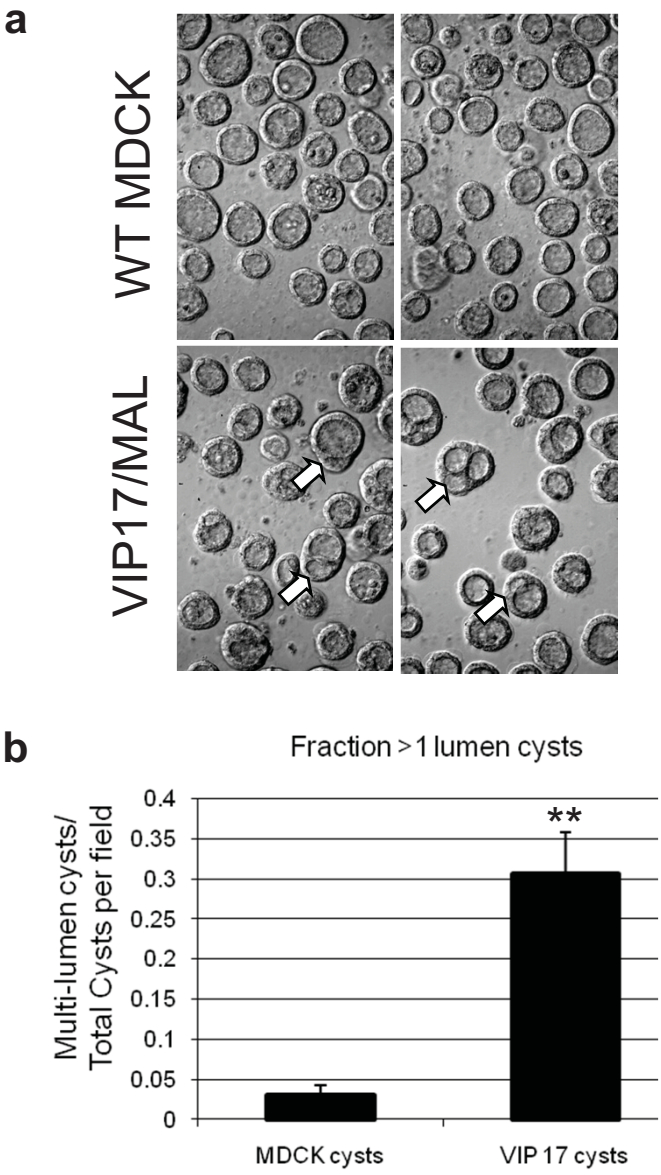
a
WT MDCK
VIP17/MAL
b
Fraction >1 lumen cysts
Multi-lumen cysts/
Total Cysts per field
0.4
0.35
0.3
0.25
0.2
0.15
0.1
0.05
0
**
MDCK cysts
VIP 17 cysts

Figure 3

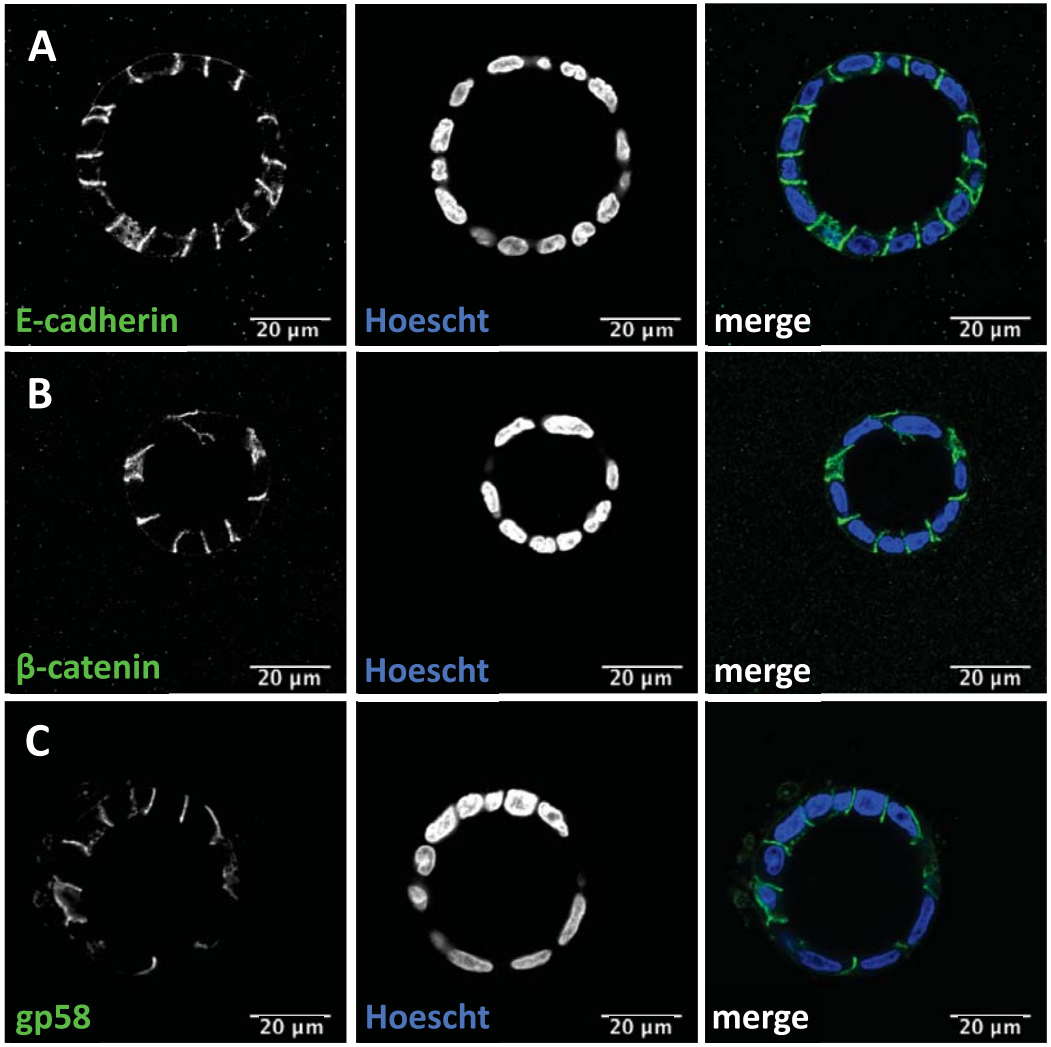
A
E-cadherin
20 µm
Hoescht
20 µm
merge
20 µm
B
β-catenin
20 µm
Hoescht
20 µm
merge
20 µm
C
gp58
20 µm
Hoescht
20 µm
merge
20 µm

Figure 4

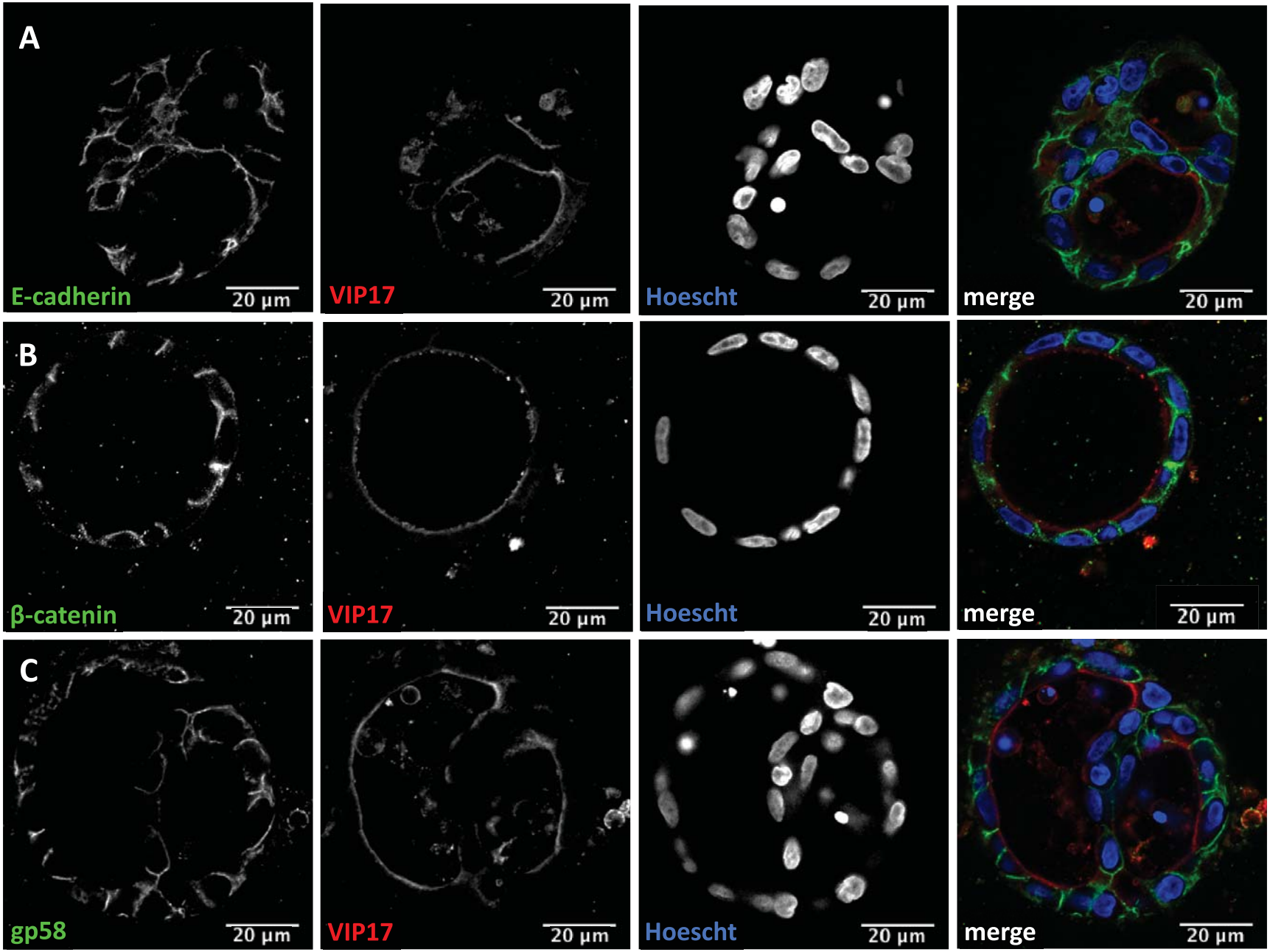
A
E-cadherin
20 µm
VIP17
20 µm
Hoescht
20 µm
merge
20 µm
B
β-catenin
20 µm
VIP17
20 µm
Hoescht
20 µm
merge
20 µm
C
gp58
20 µm
VIP17
20 µm
Hoescht
20 µm
merge
20 µm

Figure 5

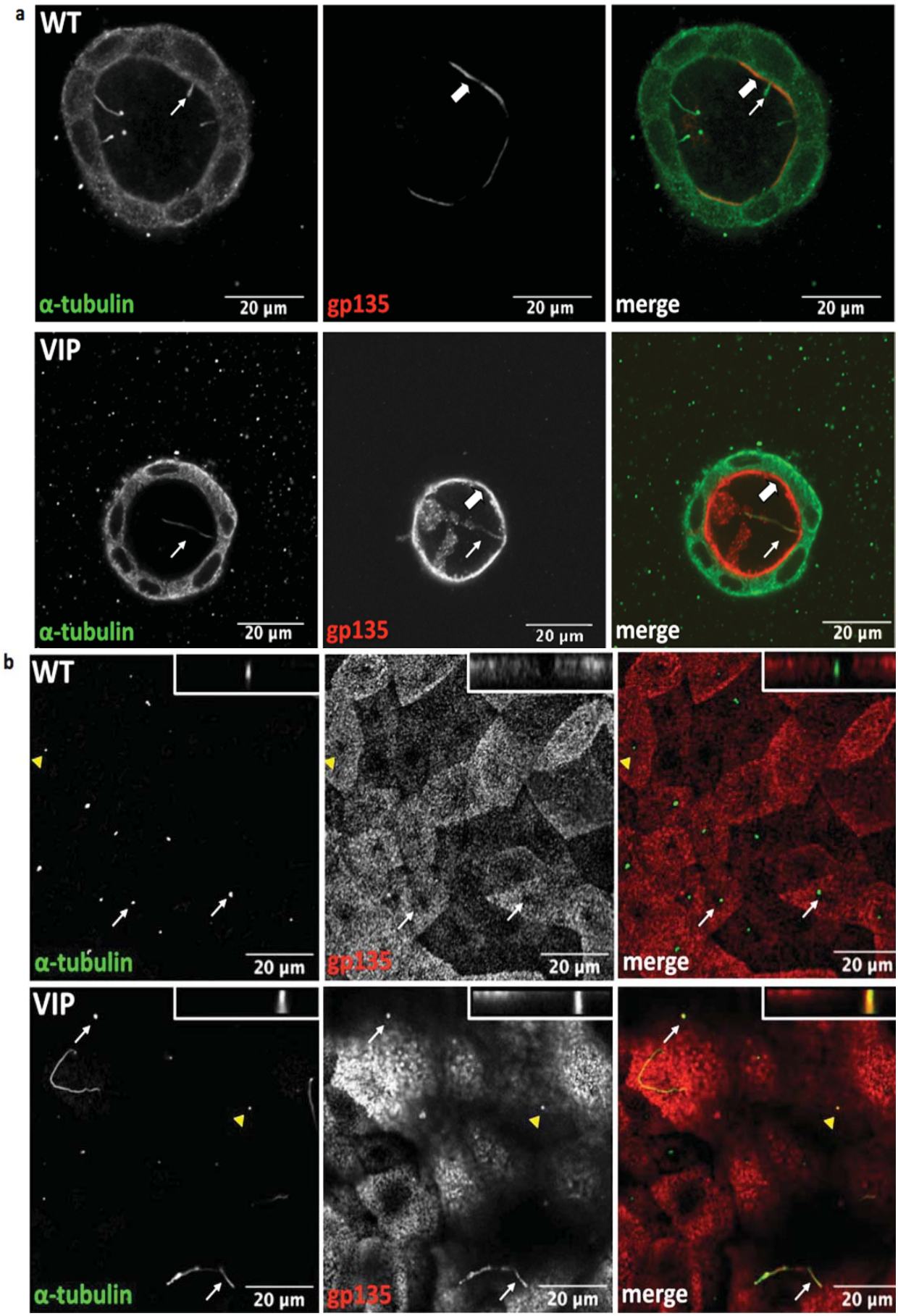
a
WT
α-tubulin
20 µm
gp135
20 µm
merge
20 µm
VIP
α-tubulin
20 µm
gp135
20 µm
merge
20 µm
b
WT
α-tubulin
20 µm
gp135
20 µm
merge
20 µm
VIP
α-tubulin
20 µm
gp135
20 µm
merge
20 µm

Figure 6

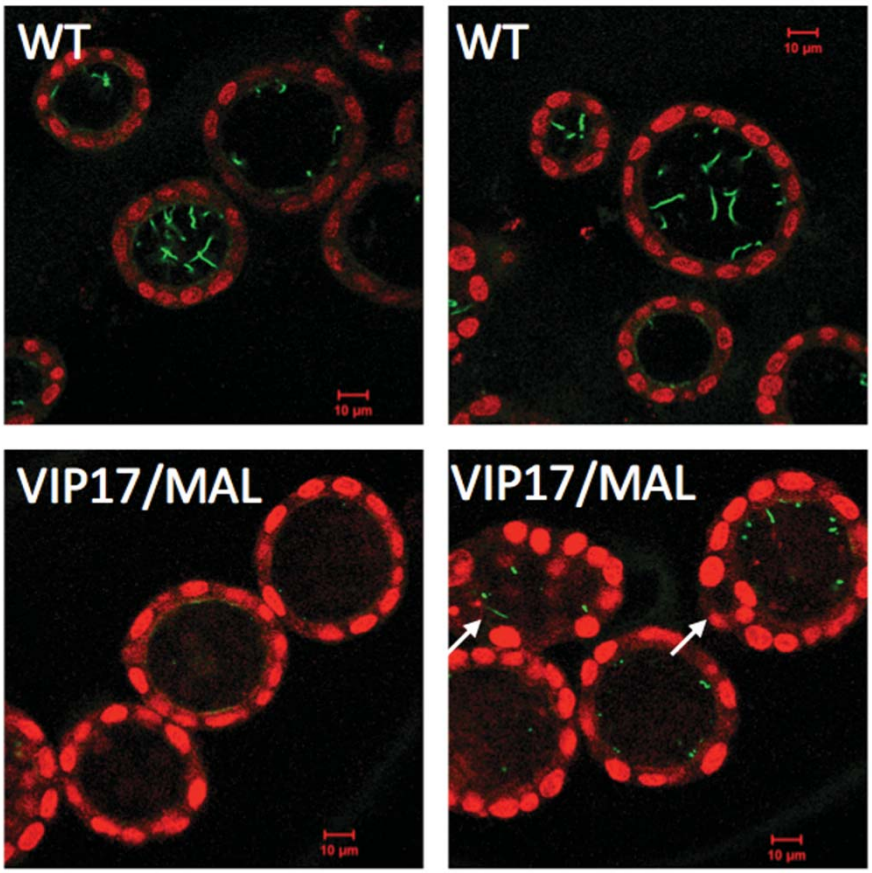

Figure 7